

## pH-dependence for binding a single nitrite ion to each type-2 copper centre in the copper-containing nitrite reductase of *Alcaligenes xylosoxidans*

Zelda H. L. ABRAHAM\*, Barry E. SMITH, Barry D. HOWES†, David J. LOWE and Robert R. EADY

Nitrogen Fixation Laboratory, John Innes Centre, Colney Lane, Norwich NR4 7UH, U.K.

The first quantitative characterization of the interaction of  $\text{NO}_2^-$  with the Cu-containing dissimilatory nitrite reductase (NiR) of *Alcaligenes xylosoxidans* using steady-state kinetics, equilibrium gel filtration and EPR spectroscopy is described. Each molecule of this protein consists of three equivalent subunits, each containing a type-1 Cu atom and also a type-2 Cu atom at each subunit interface. Enzyme activity increased in a biphasic manner with decreasing pH, having an optimum at pH 5.2 and a plateau between pH 6.1 and 5.8. Equilibrium gel filtration showed that binding of  $\text{NO}_2^-$  to the oxidized NiR was also pH-dependent. At pH 7.5, no binding was detectable, but binding was detectable at lower pH values. At pH 5.2, the concentration-dependence for binding of  $\text{NO}_2^-$  to the enzyme showed that approx. 4.1  $\text{NO}_2^-$  ions bound per trimeric NiR molecule. Unexpectedly, NiR

deficient in type-2 Cu centres bound 1.3  $\text{NO}_2^-$  ions per trimer. When corrected for this binding, a value of 3  $\text{NO}_2^-$  ions bound per trimer of NiR, equivalent to the type-2 Cu content. The  $\text{NO}_2^-$ -induced changes in the EPR parameters of the type-2 Cu centre of the oxidized enzyme showed a similar pH-dependence to that of the activity. Binding constants for  $\text{NO}_2^-$  at a single type of site, after allowing for the non-specifically bound  $\text{NO}_2^-$ , were  $350 \pm 35 \mu\text{M}$  (mean  $\pm$  S.E.M.) at pH 7.5 and  $< 30 \mu\text{M}$  at pH 5.2. The apparent  $K_m$  for  $\text{NO}_2^-$  with saturating concentrations of dithionite as reductant was  $35 \mu\text{M}$  at pH 7.5, which is 10-fold tighter than for the oxidized enzyme, and is compatible with an ordered mechanism in which the enzyme is reduced before  $\text{NO}_2^-$  binds.

### INTRODUCTION

Denitrification is the process in the nitrogen cycle in which oxyanions of nitrogen are reduced by dissimilatory reductases in a series of reactions leading to NO,  $\text{N}_2\text{O}$  or  $\text{N}_2$  gases, which are released into the atmosphere (see [1] for review). In this process, dissimilatory nitrite reductases (NiRs) catalyse the reduction of  $\text{NO}_2^-$  to NO. Two types of dissimilatory NiR are known, one containing dihaem (haem  $\text{cd}_1$ ) and the other containing Cu as the redox active centre [1,2].

The amino acid sequences of four Cu-containing NiRs have been determined, and they show a high degree of conservation (approx. 80% sequence similarity), see [3] and references therein. Most structural information is available for the enzyme of *Achromobacter cycloclastes* (AcNiR) which has been studied extensively by X-ray crystallography. The structure at 2.3 Å resolution shows a trimeric arrangement of identical subunits with a molecular mass of approx. 109 kDa. Each subunit has a type-1 Cu centre located within a typical azurin-type folding domain. The three type-2 Cu centres are positioned at the subunit interfaces and are each ligated by three histidine residues, two from one subunit and the third from an adjacent subunit [4]. An X-ray-crystallographic analysis of NiR from *Alcaligenes faecalis* S-6 (AfNiR) [5] revealed a similar arrangement of the Cu centres. Further X-ray-crystallographic studies [3] showed that  $\text{NO}_2^-$  binds via both oxygen atoms to the type-2 Cu atom, displacing a water ligand, as had been indicated by the electron nuclear double resonance (ENDOR) studies of Howes et al. [6].

The solution structure and spectroscopic properties of the dissimilatory Cu-containing NiR from *Alcaligenes xylosoxidans* subsp. *xylosoxidans* N.C.I.M.B. 11015 (AxNiR) have been characterized in detail [7,8]. This NiR, in contrast with earlier

reports [9], is a trimer of molecular mass 109 kDa containing both type-1 and type-2 Cu centres. Our EPR and ENDOR studies of this enzyme have shown that  $\text{NO}_2^-$  binds to the type-2 Cu centre to produce dramatic changes in the environment of  $^1\text{H}$  and  $^{14}\text{N}$  nuclei coupled to the type-2, but not type-1, Cu centres [6]. We have also shown, from Cu EXAFS studies, that the binding of  $\text{NO}_2^-$  to the type-2 centre results in a lengthening of the average Cu–His distance by 0.08 Å [10].

The consensus view of the mechanism of NiR when catalysing the reaction



is that the type-1 Cu centres function as electron-donor sites to the type-2 Cu centres at which  $\text{NO}_2^-$  binding and reduction occurs [3]. However, there is little direct experimental evidence for this, other than a general involvement of type-1 Cu centres in electron-transfer reactions, and the observation that  $\text{NO}_2^-$  binds to the oxidized type-2 Cu centres. Support for this proposal is provided by the properties of a mutant form of AfNiR which lacks the type-1 Cu. This mutant has no activity with reduced pseudoazurin, the presumed physiological electron donor, although it is active with electron donation from reduced Methyl Viologen [5].

Under some conditions,  $\text{N}_2\text{O}$ , in addition to NO, can be a product of the reduction of  $\text{NO}_2^-$  by Cu-containing but not haem-containing NiRs, consistent with the interaction of a second  $\text{NO}_2^-$  ion, or the reaction of the product NO, with NiR at some stage during enzyme turnover [11].

Although structural studies of  $\text{NO}_2^-$  bound to Cu-containing NiRs utilizing X-ray crystallography [3], ENDOR spectroscopy [6] and EXAFS spectroscopy [10] have been reported, this interaction has not been examined quantitatively in any detail.

Abbreviations used: NiR, nitrite reductase; ENDOR, electron nuclear double resonance; T2DNiR, type-2 Cu-deficient NiR.

\* To whom correspondence should be addressed.

† Present address: Department of Chemistry, University of Siena Pian dei Mantellini, 44, 53100 Siena, Italy.

To investigate this aspect of NiR function, we have used both the changes in the EPR parameters of the type-2 Cu centres induced by  $\text{NO}_2^-$ , and the non-spectroscopic column equilibration method of Hummel and Dryer [12] to investigate the binding of  $\text{NO}_2^-$  to oxidized NiR of *Alc. xylosoxidans* at various pH values. These data, when compared with the apparent  $K_m$  for  $\text{NO}_2^-$  reduction during enzyme turnover, are consistent with  $\text{NO}_2^-$  binding more tightly to the reduced enzyme. The relevance to the mechanism of the reduction of  $\text{NO}_2^-$  by NiR is discussed.

## EXPERIMENTAL

### Preparation of NiR and azurin

NiR and azurin I were purified from *Alc. xylosoxidans* subsp. *xylosoxidans* (N.C.I.M.B. 11015) as described by Abraham et al. [7] and Dodd et al. [13] respectively. The type-2 Cu-deficient NiR (T2DNiR) was purified using essentially the same procedures except that the activation step of adding  $\text{CuSO}_4$  to crude extracts was omitted. The specific activities using the standard assay (described below, in phosphate buffer pH 7.1) ranged from 90 to 150  $\mu\text{mol}$  of  $\text{NO}_2^-$  reduced/min per mg of protein and 20  $\mu\text{mol}$  of  $\text{NO}_2^-$  reduced/min per mg of protein for NiR and T2DNiR respectively. NiR contained  $6.2 \pm 0.3$  (mean  $\pm$  S.E.M.) Cu atoms per trimer of which approx. 50% were type-1 and 50% type-2 Cu centres [7]. T2DNiR contained  $3.8 \pm 0.4$  Cu atoms per trimer. The visible spectra of NiR and T2DNiR indicated that the type-1 Cu content of both proteins was the same, and EPR spectroscopy showed that the type-2 Cu content of T2DNiR was approx. 10% of that of NiR.

### Assay for NiR activity

#### Standard assay

During purification, NiR activity was measured at 25 °C using Methyl Viologen reduced with an excess of dithionite as described by MacGregor [14]. This is a stopped-time assay, followed by the colorimetric measurement of the amount of  $\text{NO}_2^-$  remaining in the reaction mixture [7].

In experiments to determine the pH optimum for enzymic activity, the standard buffer (50 mM phosphate, pH 7.1) was changed to a mixture of 25 mM Mes, 25 mM Hepes and 25 mM maleic acid in order to avoid the use of phosphate buffers below pH 6.6, where a significant non-enzymic loss of  $\text{NO}_2^-$  in the assay occurs, presumably because of reduction by dithionite. This mixture was titrated to give buffers over the pH range 8.0–4.0, which were used in place of the standard assay buffer. Measurements of activity were made in triplicate at each pH. No significant decomposition or non-enzymic reduction of  $\text{NO}_2^-$  occurred in this mixed-buffer system at any pH used. The specific activity of NiR at pH 7.1 in this modified assay was 45% of that measured in the standard assay containing phosphate.

#### Continuous spectrophotometric assay

In experiments to determine the apparent  $K_m$  for  $\text{NO}_2^-$ , Methyl Viologen was omitted from the assay mixture and the rate of oxidation of dithionite was followed spectrophotometrically at 315 nm ( $\epsilon$  8000  $\text{mM}^{-1}\text{cm}^{-1}$ ). The reaction mixture contained, in a final volume of 415  $\mu\text{l}$  in a 2 mm-path-length silica cuvette, 50 mM Hepes buffer, pH 7.5, containing 1 mM sodium dithionite and a range of  $\text{NO}_2^-$  concentrations up to 500  $\mu\text{M}$ . The reaction was carried out under argon and started by the injection of NiR through a rubber closure of the cuvette. At the end of the enzymic reaction, linear decomposition of dithionite continued at a rate corresponding to about 20% of the initial enzymic rate.

This linear rate was subtracted from the complete time course, which was then calibrated using the initial and final (zero) concentrations of  $\text{NO}_2^-$ , before fitting to the Michaelis–Menten equation using NAG subroutine E04FDF (NAG Ltd., Oxford, U.K.), which is used to find an unconstrained minimum of the sum of the squares of  $m$  non-linear functions in  $n$  variables.

### $\text{NO}_2^-$ binding to oxidized NiR

#### EPR measurements

EPR spectra were recorded and quantified as reported by Abraham et al. [7]. The proportion of type-2 Cu with  $\text{NO}_2^-$  bound was estimated from the height of the  $g_3$  feature at the position shown by the arrow in the top panel of Figure 5 with the heights adjusted to constant EPR integration to allow for small changes of the order of 2% caused by irreproducibility of sample positioning in the EPR spectrometer and dilution resulting from the addition of  $\text{NO}_2^-$ . The data were fitted to a curve using two binding constants, one describing  $\text{NO}_2^-$  binding to a site affecting the EPR spectrum at the concentration of the type-2 Cu, plus one at a concentration measured by equilibrium binding and having no effect on the EPR spectrum. The binding curve was generated using NAG subroutine C05NBF, which is used to find a zero of a system of  $N$  non-linear functions in  $N$  variables, and the fitting performed with NAG subroutine E04FDF.

#### Equilibrium gel filtration

To measure equilibrium binding of  $\text{NO}_2^-$  to NiR or T2DNiR, 1 ml of enzyme, initially 15 mg of protein/ml (138  $\mu\text{M}$ ), was passed through a column (0.7 cm  $\times$  10 cm) of Bio-Gel P6DG equilibrated with buffers containing various concentrations of  $\text{NO}_2^-$ . The concentration of  $\text{NO}_2^-$  in the effluent was measured colorimetrically by the method of Nicholas and Nason [15], using a calibration curve (0–1 mM) based on a standard solution of  $\text{NaNO}_2$  (EM Science associate of Merck, Darmstadt, Germany). Equilibration, before the addition of enzyme solution, was taken to be established when the concentration of  $\text{NO}_2^-$  in the effluent from the column was the same as that of the buffer applied to the column. When equilibration was established, NiR was loaded and the column effluent collected in Eppendorf tubes in approx. 250  $\mu\text{l}$  fractions; their volumes were subsequently determined by weighing. The protein concentration in each fraction (determined after diluting a 100  $\mu\text{l}$  sample to 1 ml with buffer) was determined from the  $A_{280}$  using the experimentally determined value of  $A = 1.91$  for a solution of 1 mg of NiR/ml. The total  $\text{NO}_2^-$  in each fraction was determined colorimetrically and the amount bound to NiR calculated by subtracting the baseline concentration value. The molecules of ligand bound per molecule of enzyme were calculated using a value for the molecular mass of NiR of 109 kDa [7]. The area of the trough in the elution pattern represents the depletion caused by ligand binding to protein plus that caused by the  $\text{NO}_2^-$ -free buffer applied to the column with the protein.

## RESULTS AND DISCUSSION

Steady-state kinetic studies were undertaken to determine the pH-dependence of NiR activity and apparent  $K_m$  for  $\text{NO}_2^-$  at saturating dithionite concentrations.

### pH-dependence of NiR activity

The pH-dependence of NiR activity measured using the modified mixed-buffer assay described in the Experimental section is

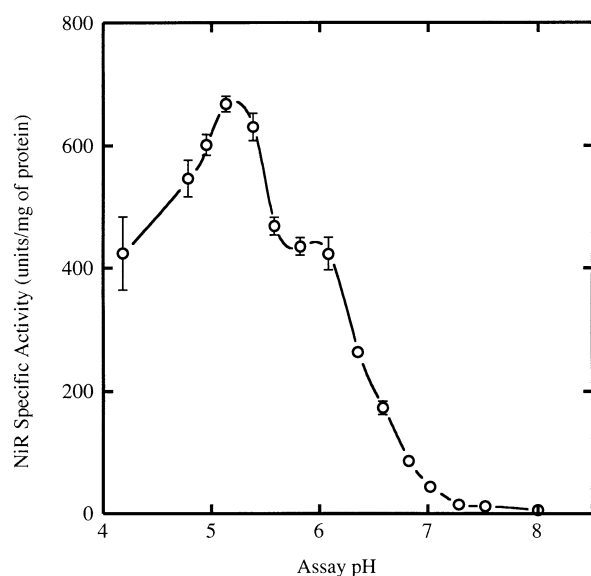


**Figure 1** pH-dependence of NiR activity

NiR activity was measured in the standard assay system [7] except that the standard buffer was replaced with a mixture of 25 mM Mes, 25 mM Hepes and 25 mM maleic acid titrated to the pH values indicated. The data shown are the means  $\pm$  S.E.M. from three determinations at each pH. The units of NiR activity are 1  $\mu$ mol of  $\text{NO}_2^-$  reduced/min at 25  $^\circ\text{C}$ .

shown in Figure 1. The activity increases with decreasing pH over the range 8.0 to 5.2, in an unusual biphasic manner, with a plateau between pH 6.1 and 5.8. The optimum pH for activity was approx. 5.2, with activity decreasing at lower pH values. This optimum is lower than the range (5.9–7) found for other NiRs [16]. Over the range of pH values from 9 to 6, our data for the activity of NiR from *Alc. xylosoxidans* are comparable with those for NiR of *Alc. faecalis* S-6 [17] and *Bacillus halodentificans* [16]. The data for the latter enzyme show an increase in activity as the pH is lowered, but do not extend below pH 6, and no optimum pH was defined. For NiR of *Alc. faecalis* S-6 the data extend to pH 5 and an optimum of pH 5.9 was determined.

In order to ensure that the data presented in Figure 1 do not arise from artifacts, control incubations were performed at each pH value. These showed that the increase in activity observed in the lower pH range was not due to the non-enzymic decomposition of  $\text{NO}_2^-$ . Similarly the decrease in activity at pH values below the optimum was not due to instability or denaturation of NiR since all reactions were linear during the assays.

The biphasic pH-dependence of NiR activity that we observe is consistent with at least two protonated groups being involved in catalysis. The X-ray crystal structures of AxNiR (F. E. Dodd, S. S. Hasnain, Z. H. L. Abraham, R. R. Eady and B. E. Smith, unpublished work) and the homologous NiRs from *Achr. cycloclastes* and *Alc. faecalis* S-6 show that there are only two non-ligand ionizable residues in the active-site cleft close to the type-2 Cu centre, His-255 and Asp-98. It has been proposed that the protonated species of His-255 has a role in hydrogen-bonding to the lone pair of a water molecule which is also hydrogen-bonded to one of the carboxylate oxygen atoms of Asp-98 [4,5]. Although it is not possible to make unambiguous assignments of residues responsible for pH-activity curves such as shown in Figure 1, it has been suggested from crystallographic studies of the  $\text{NO}_2^-$ -bound AcNiR at pH 5.4 [3] that His-255 and Asp-98 and the water bound between them are likely to be the

immediate sources of the two protons that are utilized in the reaction:



It has been proposed that cleavage of a nitrogen-oxygen bond of  $\text{NO}_2^-$  bound to the type-2 Cu atom is facilitated by the reduction of the Cu atom and donation of a proton from Asp-98 ([3]; F. E. Dodd, S. S. Hasnain, Z. H. L. Abraham, R. R. Eady and B. E. Smith, unpublished work). Our observations indicate that His-255 and Asp-98 are both likely to be protonated at the optimum pH for activity. Alternatively, residues more distant from the active site, possibly those involved in a putative proton-transfer pathway from the solvent along the 11–13 Å cleft between the subunits leading to the type-2 Cu centre, may be responsible for the observed pH effects. The protonation of  $\text{NO}_2^-$  to form  $\text{HNO}_2$  is associated with a  $\text{p}K_a$  of 3.3 at 23  $^\circ\text{C}$  and is very unlikely to account for our observations, which are consistent with  $\text{NO}_2^-$  binding to the enzyme as an anion.

### Dependence of NiR activity on $\text{NO}_2^-$ concentration

The standard assay for NiR described in [7] utilizes a stopped-time reaction followed by the colorimetric measurement of the amount of  $\text{NO}_2^-$  remaining in the reaction mixture, and, owing to the high affinity of NiR for  $\text{NO}_2^-$ , is not amenable to the determination of the apparent  $K_m$  for  $\text{NO}_2^-$ .

The continuous spectrophotometric assay for NiR activity, as described in the Experimental section, was devised to overcome this problem. This assay was based on continuous measurement of the rate of oxidation of dithionite at 315 nm during  $\text{NO}_2^-$  reduction. In the presence of saturating concentrations of  $\text{NO}_2^-$ , linear rates of dithionite oxidation were observed down to a concentration of 2  $\mu\text{M}$  dithionite, consistent with a high affinity of NiR for this reductant.

The apparent  $K_m$  for  $\text{NO}_2^-$  was determined using this assay at saturating concentrations of dithionite, and a  $\text{NO}_2^-$  concentration which was low but initially saturating. A typical progress curve is shown in Figure 2, and the apparent  $K_m$  was calculated from a series of such single progress curves. Assuming Michaelis-Menten kinetics, a good fit to the progress curve was obtained, and gave a value for the apparent  $K_m$  for  $\text{NO}_2^-$  of  $34 \pm 2 \mu\text{M}$  (mean  $\pm$  S.E.M.). No co-operativity in the interaction of  $\text{NO}_2^-$  with NiR was detected.

Consistent with our data, when a dithionite-mediated assay system was used, NiRs from a variety of denitrifying organisms gave values ranging from 35 to 74  $\mu\text{M}$  for the apparent  $K_m$  for  $\text{NO}_2^-$  [17,18]. These values indicate that under the reducing conditions of the assay, Cu-containing NiRs have a high affinity for  $\text{NO}_2^-$ . As described below, isolated oxidized NiR binds  $\text{NO}_2^-$  more weakly at this pH, consistent with an ordered mechanism during turnover in which  $\text{NO}_2^-$  binds to the reduced enzyme. This observation that  $\text{NO}_2^-$  binds to reduced enzyme is important since it is not possible to observe binding to Cu(I) by EPR/ENDOR [which can detect only the paramagnetic Cu(II)] or X-ray crystallography (since the  $\text{NO}_2^-$  would be rapidly reduced on the time scale of such measurements).

### Equilibrium binding of $\text{NO}_2^-$ to oxidized NiR

This method was used to investigate the interaction of NiR with  $\text{NO}_2^-$  independently of any spectroscopic property. Purified NiR was chromatographed on columns that had been pre-equilibrated

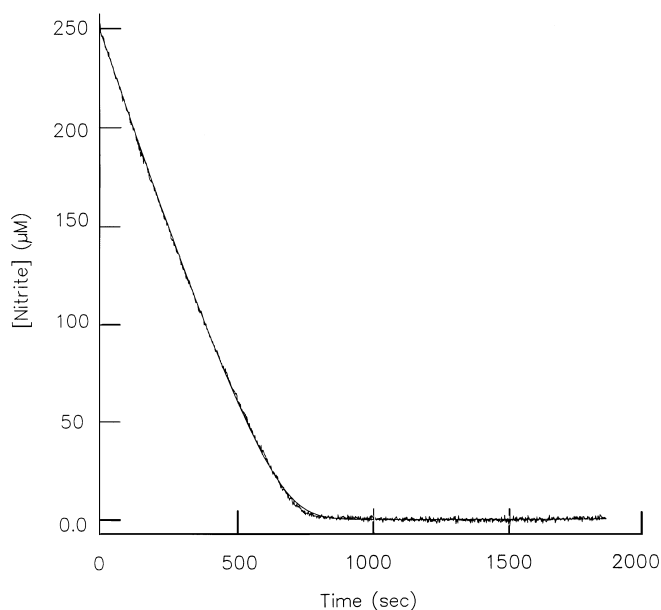


**Figure 2** Progress curve for the oxidation of sodium dithionite by NiR

The assay conditions are those of the standard assay except that Methyl Viologen was omitted, and the progress of the reaction of NiR-dependent oxidation of sodium dithionite was monitored spectrophotometrically at 315 nm in a sealed cuvette under  $N_2$ . Sodium dithionite at 1 mM was saturating and a range of limiting  $NO_2^-$  concentrations was used up to 500  $\mu M$ . The time course fitted to Michaelis–Menten kinetics as described in the Experimental section is shown as the solid line. In this Figure the initial concentration of  $NO_2^-$  was 250  $\mu M$ . Note that the rate becomes non-linear at  $\sim 100 \mu M NO_2^-$ , at which concentration  $NO_2^-$  is no longer saturating.

with  $NO_2^-$  at concentrations over the range 50–2000  $\mu M$ . At pH 7.5, the interaction of  $NO_2^-$  with the enzyme was too weak to be detected using the column-equilibration method (Figure 3A). However, at pH 6.0 or 5.2 using 100  $\mu M NO_2^-$ , tighter binding was observed, because  $NO_2^-$  bound to NiR could be detected colorimetrically in the void volume of the column as a peak coincident with the protein-elution profile determined from  $A_{280}$  (Figures 3B and 3C). These data show that at an  $NO_2^-$  concentration of 100  $\mu M$ , significantly more  $NO_2^-$  was bound to NiR at pH 5.2 than at pH 6.0. In fractions following the peak of NiR, the concentration of  $NO_2^-$  returned rapidly to the basal concentration, indicating rapid equilibrium binding of substrate to the enzyme. Consistent with this, when NiR with  $NO_2^-$  bound was chromatographed on a column equilibrated with buffer that did not contain  $NO_2^-$ , NiR could be separated from the  $NO_2^-$ .

The stoichiometry of  $NO_2^-$  binding to NiR was investigated at pH 5.2, using this technique, over the concentration range 50–2000  $\mu M NO_2^-$ . Saturation binding was observed with a limiting value of  $4.1 \pm 0.4 NO_2^-$  ions per trimer of NiR (Figure 4), but the shape of the curve suggests the presence of two classes of binding site. The value of 4.1  $NO_2^-$  ions per trimer of NiR is significantly higher than would be expected for a single  $NO_2^-$  ion binding to each of the three type-2 Cu centres.

This discrepancy was resolved when similar binding experiments were carried out with NiR essentially lacking type-2 Cu (T2DNiR). Surprisingly, this species of the enzyme bound  $1.3 \pm 0.2 NO_2^-$  ions per trimer at pH 5.2 (Figure 4), with saturation occurring at  $\sim 500 \mu M$ . The binding of  $NO_2^-$  to T2DNiR has not been reported previously. However, this is the first study in which gel equilibration has been utilized to investigate binding directly rather than using changes in spec-

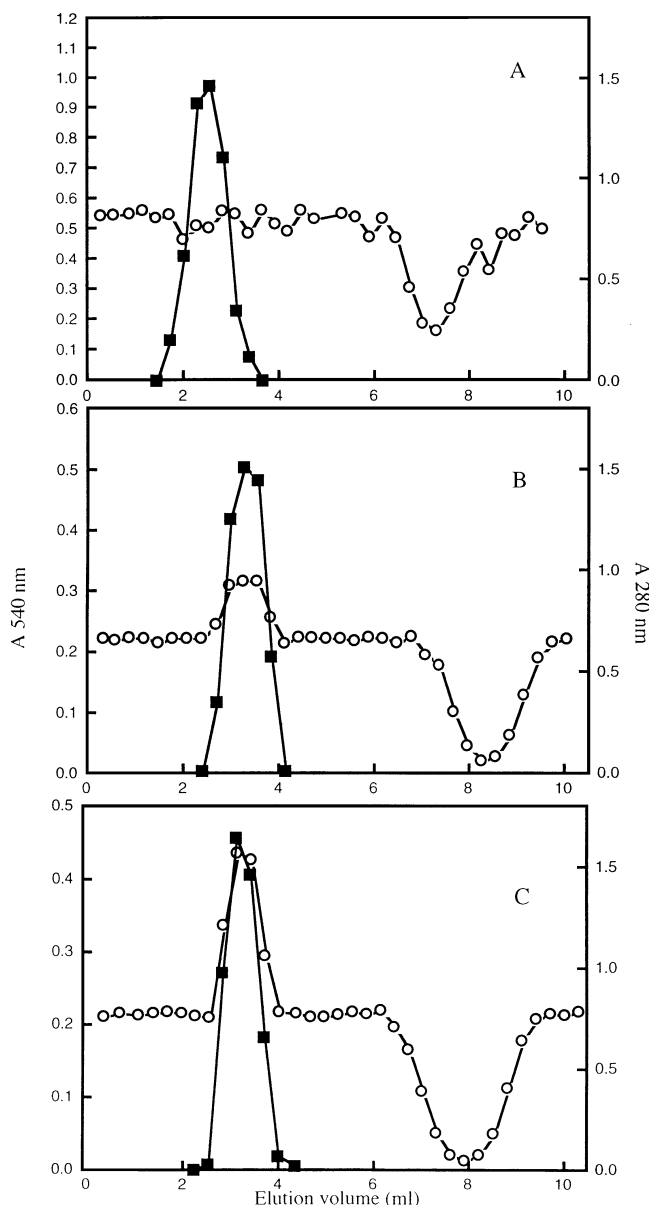


**Figure 3** Measurement of  $NO_2^-$  binding to NiR using gel-permeation chromatography

Binding of  $NO_2^-$  to NiR was measured by the gel-permeation method [12] as described in the Experimental section. The column was equilibrated with (A) 250  $\mu M NO_2^-$  in Hepes buffer, pH 7.5, (B) 100  $\mu M NO_2^-$  in Mes buffer, pH 6.0, (C) 100  $\mu M NO_2^-$  in Mes buffer, pH 5.2. NiR (1 ml; 15 mg/ml protein) was loaded on to a column (0.7 cm  $\times$  10 cm) of Bio-Gel P6DG equilibrated with the buffers indicated above, fractions were collected and  $A_{280}$  (■) was measured to determine the concentration of NiR, after dilution of a 100  $\mu l$  sample from each fraction with buffer to 1 ml total volume. The  $NO_2^-$  concentrations (○) of the tube contents were determined colorimetrically after dilution of a 50  $\mu l$  sample from each fraction with buffer to 100  $\mu l$  total volume. The post-protein trough in (A) is due to depletion of  $NO_2^-$  in the loading volume of the sample, and in (B) and (C) is due to this depletion and also to  $NO_2^-$  bound to NiR. Under the conditions of (B) and (C) the  $NO_2^-$  bound to NiR was calculated by subtraction of the basal level from the concentration of  $NO_2^-$  in the tubes containing NiR.

troscopic parameters of the Cu centres. From Figure 4 it is clear that, at the two lowest concentrations of  $NO_2^-$  tested, NiR binds significantly more  $NO_2^-$  than does T2DNiR at pH 5.2. No binding to T2DNiR was detectable at pH 7.5 over this range of  $NO_2^-$  concentrations using the gel-binding method. The presence

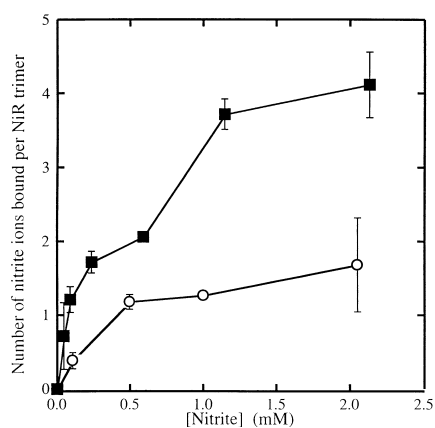


**Figure 4** Concentration-dependence of the amount of  $\text{NO}_2^-$  bound to NiR

The amount of  $\text{NO}_2^-$  bound to NiR (■) and T2DNiR (○) in Mes buffer, pH 5.2, was determined at initial  $\text{NO}_2^-$  concentrations in the range 50–2000  $\mu\text{M}$  as described in Figure 3.

of this previously undetected binding site on NiR readily accounts for the  $\text{NO}_2^-$  bound in excess of the type-2 Cu content of the enzyme.

In these binding experiments it is not possible to estimate apparent dissociation constants from the data presented in Figure 4, because the NiR-binding site concentration used was necessarily, for experimental reasons, close to that of  $\text{NO}_2^-$  resulting in a significant decrease in the free ligand concentration. However,

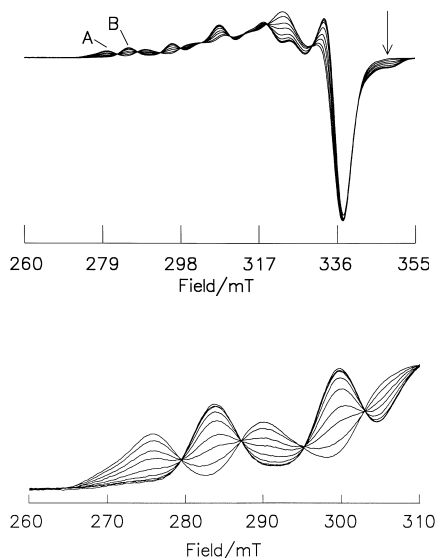


**Figure 5** EPR spectra of NiR during titration with  $\text{NO}_2^-$

Various volumes of  $\text{NaNO}_2$  solution up to a final concentration of 5 mM were added to NiR in 25 mM Mes buffer, pH 5.2. Spectra were normalized to the same integrated intensity to account for the dilution occurring as the  $\text{NO}_2^-$  solution was added. Top, complete EPR spectra where A is NiR alone and B is NiR in the presence of excess  $\text{NO}_2^-$ . Bottom, expansion of the low-field part of the spectra demonstrating that only two species contribute to the type-2 Cu EPR spectrum as it was converted from the free to the  $\text{NO}_2^-$ -bound form. The arrow in the top panel shows where the measurements plotted in Figure 6 were taken. EPR running conditions were: temperature 100 K; microwave power 10 mW at 9.412 GHz; modulation amplitude 0.49 mT at 100 KHz.

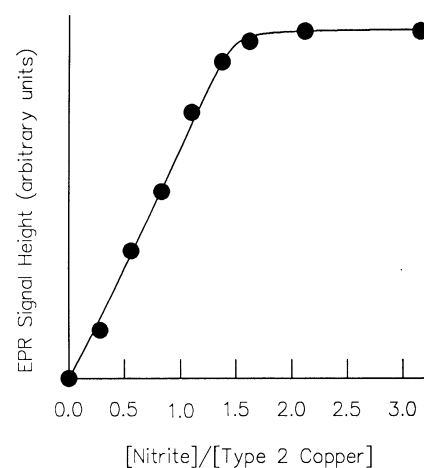


**Figure 6** Titration of NiR with  $\text{NO}_2^-$  monitored by EPR

The points are signal heights at the position indicated by the arrow in the EPR traces of the top panel of Figure 5. The curve shows a fit to the data with one binding site per type-2 Cu centre as determined from the integrated EPR intensity plus one Cu-independent site per trimeric molecule as defined in the Experimental section, and uses binding constants of 7.0 and 5.3  $\mu\text{M}$  respectively.

the shape of the curve implies tight binding consistent with our EPR data (see below).

Several experimental approaches have shown that the structure of NiR is not significantly perturbed by the loss of Cu from the type-2 site. Solution small-angle X-ray scattering of AxT2DNiR [10] and an X-ray crystallographic study of AcT2DNiR [3] have shown that the loss of the Cu from this centre, which is at the interface of the subunits, has very little effect on the structure of the enzyme. EPR and ENDOR studies of AxT2DNiR have shown that even at 1 M  $\text{NO}_2^-$  only very small changes occur at the type-1 Cu centre. The observed effects are too small to arise from  $\text{NO}_2^-$  binding directly at this centre, but may possibly arise from a small perturbation when  $\text{NO}_2^-$  binds to the adjacent type-2 Cu.

The binding of  $\text{NO}_2^-$  to azurin I, a small type-1 Cu-containing protein, was also measured by this method using 1 mM  $\text{NO}_2^-$  at pH 5.2 (results not shown). On a per mg of protein basis, azurin bound  $\text{NO}_2^-$  to the same extent as T2DNiR; however, on a molar basis, only 0.12  $\text{NO}_2^-$  ions were calculated to bind per azurin molecule compared with 1.3 for T2DNiR. This may indicate that there is some non-specific binding of  $\text{NO}_2^-$  to these proteins at pH 5.2. An EXAFS study previously demonstrated that  $\text{NO}_2^-$  does not interact with the type-1 Cu centre in T2DNiR at pH 6.0 [10].

#### Binding of $\text{NO}_2^-$ to NiR monitored by EPR spectroscopy

When  $\text{NO}_2^-$  binds to NiR, the EPR spectrum of the type-2 Cu(II) shows a decrease in  $g_{\parallel}$  and an increase in  $A_{\parallel}$  [6]. Figure 5 (top) shows the EPR spectra of NiR alone (A) and in the presence of excess  $\text{NO}_2^-$  (B), and also shows the stages in the transition of A to B as the concentration of  $\text{NO}_2^-$  is increased. Figure 5 (bottom) shows an expansion of the low-field region of these spectra. The presence of the isoclinics in the spectra at low field, due to the type-2 copper alone, show that only two species of this centre are involved. Thus these changes allow the binding of  $\text{NO}_2^-$  to NiR to be monitored (Figure 6).

The concentration-dependence of the  $\text{NO}_2^-$ -induced changes in the EPR spectra showed non-ideal behaviour at low  $\text{NO}_2^-$

concentrations, particularly apparent at pH 5.2. However, the binding studies of T2DNIr discussed above indicate the presence of a binding site present at  $\sim 0.4$  sites per type-2 Cu centre. When the contribution of this EPR-undetectable binding site was taken into account, the analysis of the EPR data gave a good fit to the non-co-operative binding of one  $\text{NO}_2^-$  per type-2 Cu centre consistent with the gel equilibrium-binding data. Non-co-operativity is consistent with the apparent  $K_m$  data, indicating that, although the EXAFS and ENDOR data show that the structure of the type-2 Cu centre changes geometry when  $\text{NO}_2^-$  binds [6,10], the three centres behave independently.

An analysis of the binding curves for the  $\text{NO}_2^-$ -induced change in the type-2 Cu(II) EPR gave best-fit binding constants of  $350 \pm 35 \mu\text{M}$  at pH 7.5 and  $7.0 \pm 0.7 \mu\text{M}$  at pH 5.2 (means  $\pm$  S.E.M.). The EPR non-detectable  $\text{NO}_2^-$ -binding site, also evident from the gel equilibration studies, had no effect on the fit at pH 7.5, but, when taken into account in analysing the data at pH 5.2, gave a binding constant of  $5.3 \pm 0.5 \mu\text{M}$ . However, the value at pH 5.2 depends critically on the accuracy to which the type-2 Cu content can be determined (approx. 10%). Fitting of the curves assuming a 10% error gave values up to  $27 \mu\text{M}$ ; because of this uncertainty we regard the value at pH 5.2 to be  $< 30 \mu\text{M}$ . Fitting of the binding curves ignoring the Cu-independent binding site gave the same value within experimental error at pH 7.5, since the EPR-detectable site shows relatively weak binding. However, at pH 5.2 such fits were significantly worse and gave curves showing systematic deviations from the data when no correction for this binding was made.

### Mechanistic implications

These investigations show that the binding of  $\text{NO}_2^-$  to isolated NiR is pH-dependent, the binding constant becoming  $\sim 10$ -fold tighter as the pH is lowered from 7.5 to 5.2. Both the EPR spectroscopy and gel equilibration binding data described above show that one  $\text{NO}_2^-$  ion binds to each type-2 Cu centre of oxidized AxNiR. The formation of  $\text{N}_2\text{O}$  during turnover of Cu-containing NiRs under some conditions [11] does not appear to involve the binding of two  $\text{NO}_2^-$  ions to oxidized type-2 Cu centres and is therefore consistent with it being formed by the further reaction of NO, formed by the reduction of  $\text{NO}_2^-$ , with a Cu nitrosyl intermediate [11].

We also show that the pH-dependence of AxNiR activity is biphasic with an optimum at 5.2 and a plateau between 6.1 and 5.8, indicating the involvement of at least two protonation events. The nature of the group(s) which become protonated and are responsible for this tighter binding to oxidized NiR are likely to be residues close to the type-2 Cu centres. Adman et al. [3] proposed from X-ray-crystallographic studies of AcNiR that Asp-98 and His-255 were the most probable sources of protons required for  $\text{NO}_2^-$  reduction. In the case of AxNiR, the binding of  $\text{NO}_2^-$  to oxidized NiR occurs at a type-2 Cu atom, with hydrogen-bonding between an oxygen atom of the  $\text{NO}_2^-$  and Asp-98 at a distance of 3.4 Å (F. E. Dodd, S. S. Hasnain, Z. H. L. Abraham, R. R. Eady and B. E. Smith, unpublished work). Thus it is likely that Asp-98 is one of those residues involved in the pH response that we observe. In this context it should be noted that no significant structural changes ( $< \text{about } 0.18 \text{ \AA}$ ) were observed for the AcNiR by X-ray crystallography as the pH was lowered

from 6.8 to 5.0 [3], so that the tighter binding at lower pH must be related to very subtle structural changes; note that the pH optimum of AcNiR has been measured as 6.2 [19] but no data were presented.

The binding of  $\text{NO}_2^-$  to NiR has been proposed to occur by displacement of a water molecule from the type-2 Cu atom [6]. This replacement would be facilitated by factors that could potentially stabilize the water molecule within the active-site cleft by hydrogen-bonding. In the X-ray-crystal structures of AxNiR (F. E. Dodd, S. S. Hasnain, Z. H. L. Abraham, R. R. Eady and B. E. Smith, unpublished work) and AcNiR [3], His-255 is situated in the solvent channel, and a role for this residue in water stabilization has been proposed.

The apparent  $K_m$  of NiR for  $\text{NO}_2^-$  at pH 7.5 is some 10-fold tighter than that determined for the oxidized protein from EPR measurements at the same pH. This indicates that effective binding leading to substrate reduction is likely to involve a reduced NiR species generated under turnover conditions. In dithionite-mediated assays electron donation occurs directly to the type-2 Cu site [5], and our findings are compatible with an ordered mechanism predominating under these conditions where reduction of this centre precedes the binding of  $\text{NO}_2^-$ .

We gratefully acknowledge Dr. R. W. Miller for useful discussions and Mr. T. Brüser for experimental assistance with part of this work. We also acknowledge the BBSRC and EU HCM Network MASIMO ERBCHRXCT920072 for provision of financial support.

### REFERENCES

- Zumft, W. G. (1992) in *The Prokaryotes*, vol. 1 (Barlows, A., Trüper, H. G., Dworkin, M., Harder, W. and Schliefer, H. K., eds.), 2nd edn., pp. 534–553, Springer-Verlag, New York
- Berks, B. C., Ferguson, S. J., Moir, J. W. B. and Richardson, D. J. (1995) *Biochim. Biophys. Acta* **1232**, 97–173
- Adman, E. T., Godden, J. W. and Turley, S. (1995) *J. Biol. Chem.* **46**, 27458–27474
- Godden, J. W., Turley, S., Teller, D. C., Adman, E. T., Liu, M. Y., Payne, W. J. and LeGall, J. (1991) *Science* **253**, 438–442
- Kukimoto, M., Nishiyama, M., Murphy, M. E. P., Turley, S., Adman, E. T., Horinouchi, S. and Beppu, T. (1994) *Biochemistry* **33**, 5246–5252
- Howes, B. D., Abraham, Z. H. L., Lowe, D. J., Brüser, T., Eady, R. R. and Smith, B. E. (1994) *Biochemistry* **33**, 3171–3177
- Abraham, Z. H. L., Lowe, D. J. and Smith, B. E. (1993) *Biochem. J.* **295**, 587–593
- Grossman, G. J., Abraham, Z. H. L., Adman, E. T., Neu, M., Eady, R. R., Smith, B. E. and Hasnain, S. S. (1993) *Biochemistry* **32**, 7360–7366
- Masuko, M., Iwasaki, H., Sakurai, T., Suzuki, S. and Nakahara, A. (1984) *J. Biochem. (Tokyo)* **96**, 447–454
- Strange, R. W., Dodd, F. E., Abraham, Z. H. L., Grossmann, J. G., Brüser, T., Eady, R. R., Smith, B. E. and Hasnain, S. S. (1995) *Struct. Biol.* **2**, 287–292
- Jackson, M. A., Tiedje, J. M. and Averill, B. A. (1991) *FEBS Lett.* **291**, 41–44
- Hummel, J. P. and Dryer, W. J. (1962) *Biochim. Biophys. Acta* **63**, 530–532
- Dodd, F. E., Hasnain, S. S., Hunter, W. N., Abraham, Z. H. L., Debenham, M., Kanzler, H., Eldridge, M., Eady, R. R., Ambler, R. P. and Smith, B. E. (1995) *Biochemistry* **34**, 10180–10186
- MacGregor, C. H. (1978) *Methods Enzymol.* **53**, 347–355
- Nicholas, D. J. D. and Nason, A. (1957) *Methods Enzymol.* **3**, 981–984
- Denariáz, G., Payne, W. J. and LeGall, J. (1991) *Biochim. Biophys. Acta* **1056**, 225–232
- Kakutani, T., Watanabe, H., Arima, K. and Beppu, T. (1981) *J. Biochem. (Tokyo)* **89**, 453–461
- Michalski, W. P. and Nicholas, D. J. D. (1985) *Biochim. Biophys. Acta* **828**, 130–137
- Iwasaki, H., Noji, S. and Shidara, S. (1975) *J. Biochem. (Tokyo)* **78**, 355–361